



HAL
open science

Magnetic and elemental characterization of the particulate matter deposited on leaves of urban trees in Santiago, Chile

M. Préndez, C. Carvallo, N. Godoy, C. Egas, B. Aguilar Reyes, G. Calzolari,
R. Fuentealba, F. Lucarelli, S. Nava

► **To cite this version:**

M. Préndez, C. Carvallo, N. Godoy, C. Egas, B. Aguilar Reyes, et al.. Magnetic and elemental characterization of the particulate matter deposited on leaves of urban trees in Santiago, Chile. *Environmental Geochemistry and Health*, 2022, 10.1007/s10653-022-01367-w . hal-03844081

HAL Id: hal-03844081

<https://hal.science/hal-03844081v1>

Submitted on 8 Nov 2022

HAL is a multi-disciplinary open access archive for the deposit and dissemination of scientific research documents, whether they are published or not. The documents may come from teaching and research institutions in France or abroad, or from public or private research centers.

L'archive ouverte pluridisciplinaire **HAL**, est destinée au dépôt et à la diffusion de documents scientifiques de niveau recherche, publiés ou non, émanant des établissements d'enseignement et de recherche français ou étrangers, des laboratoires publics ou privés.

1 **MAGNETIC AND ELEMENTAL CHARACTERIZATION OF THE**
2 **PARTICULATE MATTER DEPOSITED ON LEAVES OF URBAN TREES IN**
3 **SANTIAGO, CHILE.**

4

5 M. Préndez¹, C. Carvallo*², N. Godoy¹, C. Egas³, B.O. Aguilar Reyes⁴, G. Calzolari⁵, R.
6 Fuentealba¹, F. Lucarelli⁵, S. Nava⁵

7

8 ¹Universidad de Chile, Facultad de Ciencias Químicas y Farmacéuticas, Sergio Livingtone
9 1007, Independencia, Santiago, Chile.

10 ²Sorbonne Université, UMR 7590, Institut de Minéralogie, de Physique des Matériaux et de
11 Cosmochimie, 4 Place Jussieu, 75005 Paris, France. Email : claire.carvallo@sorbonne-
12 [universite.fr](mailto:claire.carvallo@sorbonne-universite.fr)

13 ³Universidad de Talca, Instituto Ciencias Biológicas, Av Lircay s/n, Talca, Chile.

14 ⁴Unidad Morelia, Instituto de Investigaciones en Materiales, Universidad Nacional
15 Autónoma de México, Antigua carretera a Pátzcuaro No 8701, Col. Ex Hacienda de San
16 José de la Huerta, 58190 Morelia, Michoacán, México.

17 ⁵Department of Physics and Astronomy, University of Florence and National Institute of
18 Nuclear Physics (INFN), Florence, Italy.

19

20 **Statements and declarations**

21 The authors have no relevant financial or non-financial interests to disclose. The authors have no
22 conflicts of interest to declare that are relevant to the content of this article. All authors certify that
23 they have no affiliations with or involvement in any organization or entity with any financial interest
24 or non-financial interest in the subject matter or materials discussed in this manuscript. The authors
25 have no financial or proprietary interests in any material discussed in this article.

26
27 All authors contributed to the study conception and design. Sampling was performed by C. Egas, N.
28 Godoy and M. Préndez. Magnetic measurements and analysis were carried out by C. Egas, C.
29 Carvallo and B. Aguilar, PIXE measurements and analysis by R. Fuentealba, F. Lucarelli, G. Calzolari
30 and S. Nava. The first draft of the manuscript was written by M. Préndez and C. Carvallo, with
31 artwork by N. Godoy and C. Egas, and all authors commented on previous versions of the manuscript.
32 All authors read and approved the final manuscript.

33 This study did not involve any humans or animal subjects. This manuscript does not contain any
34 individual person's data.

35

36 The datasets generated during and/or analysed during the current study are available from the
37 corresponding author on reasonable request.

38 **Abstract**

39 Airborne particulate matter is a serious threat to human health, especially in fast-growing cities. In
40 this study, we carried out a magnetic and elemental study on tree leaves used as passive captors and
41 urban dust from various sites in the city of Santiago, Chile, to assess the reliability of magnetic and
42 elemental measurements to characterize particulate matter pollution. We found that the magnetic
43 susceptibility and saturation isothermal remanent magnetization measured on urban tree leaves is a
44 good proxy for tracing anthropogenic metallic particles and allow controlling the exposure time for
45 particulate matter collection. Similar measurements on urban soil can be influenced by particles of
46 detritic (natural) origin, and therefore, magnetic measurements on tree leaves can help to identify
47 hotspots where fine particles are more abundant. Elemental Particle Induced X-ray Emission (PIXE)
48 analysis of tree leaves showed the presence of a number of elements associated with vehicular
49 emissions, in particular Cu, Zn, Fe, K and S which are present at every site, and As, Se, V, Ni, Sr, Zr,
50 Mo and Pb identified at some sites. We observed a correlation between magnetic parameters and the
51 concentrations of S and Br as well as Cu to a smaller extent. Moreover, this study shows the
52 importance of selecting carefully the tree species as well as the location of trees in order to optimize
53 phytoremediation.

54

55 Keywords: Urban air pollution; vehicular emissions; magnetic characterization; PIXE elemental
56 quantification; urban vegetation; phytoremediation

57

58

59 I- Introduction

60

61 The increase in the urban population leads to the loss of natural landscape and its replacement by an
62 artificially built environment; it is a global phenomenon, greater in Latin America. Consequently,
63 urban air quality has been deteriorating and many cities currently experience pollution levels above
64 the World Health Organization (WHO) recommended limits. Among others, particulate matter (PM)
65 is a frequently found contaminant in cities. It is present in the atmosphere with different mass
66 concentrations, sizes, shapes and chemical composition, because it comes from many different
67 sources, atmospheric conditions and urban geometry in relatively small areas (Buccolieri et al., 2010;
68 Hofman et al., 2013). Both acute and chronic exposure to inhalable particles PM with aerodynamic
69 diameter $\leq 10 \mu\text{m}$ (PM_{10}) is associated with various pulmonary, cardiovascular and neurological
70 problems (Pope and Dockery, 2006; Costa et al., 2014; Weichenthal et al., 2017; Coccini et al., 2017;
71 Liu et al., 2018; Malik et al., 2019).

72 In cities such as Santiago, the main sources of anthropogenic PM are vehicle usage, industrial
73 activities and emissions from burning fossil fuel and wood. In many countries, both the mass
74 concentrations of PM_{10} and $\text{PM}_{2.5}$ (fine inhalable particles with aerodynamic diameter $\leq 2.5 \mu\text{m}$) are
75 included in the standardized outdoor air quality measurement. In Santiago, this monitoring is carried
76 out with 11 stations managed by the Ministry of the Environment's air quality monitoring network
77 (SINCA). However, many urban areas lack coverage and the network cannot characterize the
78 temporal and spatial variability of PM concentrations (Karner et al., 2010; Zikova et al., 2017),
79 hindering the estimation of exposure to PM and its effects in health, or the understanding of the
80 effectiveness of emission reduction policies (Kelly et al., 2017; Tsai et al., 2019). Moreover, the
81 ultrafine particles (UFP: fine inhalable particles with aerodynamic diameter $\leq 0.1 \mu\text{m}$) are not
82 considered in this monitoring. In Chile, particularly Santiago, concentrations of PM are especially
83 high during critical episodes of pollution occurring in autumn-winter seasons (Préndez et al., 2011;
84 Toro et al., 2014).

85 However, there is growing evidence that the removal of PM is one of the positive effects of urban
86 forests (Dzierzanowski et al., 2011; Song et al., 2015; Manes et al., 2016; Nowak et al., 2018), among
87 other effects such as providing primary productivity of vegetation (Costanza et al., 2007; Roeland et
88 al., 2019) or removing gases (Nowak et al., 2018; Araya et al., 2019). Indeed, the leaves' surface and
89 stems adsorb or absorb significant amounts of air pollutants. Although a fraction of this PM is
90 resuspended by wind, another part remains attached to the plant. Moreover, particles with
91 aerodynamic size less than 0.2 μm can be captured by the leaves through the stomata (Ottel  et al.,
92 2010; Song et al., 2015). The effectiveness of this effect is species-specific. Dzierzanowski et al.
93 (2011) showed that four species of roadside trees-were able to purify urban air by dry deposition of
94 PM on the leaves.

95 However, urban trees in Santiago are mainly exotic species (~86%), which lose their leaves in the
96 autumn-winter period (Hern andez & Villase nor, 2018) of highest PM concentrations and therefore
97 have little contribution to the PM decontamination process when it is most needed.

98 The quantification of PM in urban environment can be achieved using magnetic measurements (e.g.,
99 Matzka and Maher, 1999). Indeed, magnetic particles are present in PM from vehicular sources,
100 because particles emitted as residuals from fuel burning and wear and friction of engine components
101 are Fe-rich. These particles can also lodge in their structure other toxic metals such as Pb, Zn, Ba, Cd
102 and Cr because of the affinity of Fe oxides with trace metals (Aguilar Reyes et al., 2011, 2013; Cao
103 et al., 2015). Several studies have reported a good correlation between magnetic susceptibility and
104 the heavy metal content (Mitchell and Maher, 2009; Aguilar Reyes et al., 2010; Wang, 2013; Yang
105 et al., 2017). As a consequence, the magnetic method has been developed to provide a fast and
106 inexpensive alternative for monitoring metallic fine particles in anthropogenic pollution, especially
107 those coming from transport. The use of biological passive captors (tree leaves, bark, lichens, and
108 moss) has been popularized because they are widely available in cities, sampled at breathing height,
109 and provide a record of location-specific and time-integrated information on local air quality. A

110 number of magnetic biomonitoring studies have been carried out recently in Latin American cities
111 using such captors (e.g., Chaparro et al., 2013; Marié et al., 2016; Castaneda-Miranda et al., 2021).
112 The principal source of pollution by PM in Santiago is vehicular pollution (Gramsch et al., 2014).
113 Moreover, other studies have shown that roadside tree leaves are mainly sensitive to the effect of
114 vehicular pollution (e.g., Matzka and Maher, 1999; Moreno et al., 2003; Muñoz et al., 2017). Our
115 study was divided into three subparts with different goals:

- 116 - To study spatial variation of PM along a section of a busy avenue
- 117 - To evaluate the ability of several tree species present in Santiago in trapping PM
- 118 - To assess the relevance of Air Official Monitoring Stations (AOMS) location by comparing
119 the measurements close to the AOMS with measurements from the other two subparts.

120 These goals are addressed by means of standard magnetic measurement and in some cases elemental
121 measurements, on tree leaves. Urban dust was also studied in some cases in combination with the tree
122 leaves.

123

124 **II- Materials and methods**

125 **II.1 Sampling**

126 Santiago City is located in the Metropolitan Region and counts more than 8 million inhabitants. The
127 chosen sampling sites are in the area (2 km of radius) covered by the air official monitoring stations
128 (AOMS) installed in 11 Santiago communes.

129 At each site, 10-15 mature and well exposed leaves were collected per tree at a height of about 1.75
130 m. When available, urban dust (UD), was swept from the asphalt close to the sampled trees (see
131 Supplementary Information (SI) section for more details). The sampling was conducted over three
132 campaigns.

133 The 27 leaves samples and the 17 UD samples were organized into three groups (Fig.1, Table SI-1):

134 A) Recoleta group corresponding to leaves of ten individuals of *Acer negundo* and UD along Recoleta
135 Avenue (north of the capital), all sampled on the same day. B) Mixed tree species group

136 corresponding to eight samples of *Olea europeae*, *Brachichyton populneus*, *Quillaja saponaria*,
137 *Schinus molle*, *Cryptocaria alba*, *Acacia caven* and *Maytenus boaria* (one sample for each species),
138 and the UD from streets and avenue in front of the trees, all sampled on the same day . C). Air Official
139 Monitoring Stations (AOMS) group corresponding to nine young individuals of *Quillaja saponaria*
140 near nine AOMS (situated between 2 and 700 m from AOMS, but between 2 and 30 m from the
141 street). They were sampled between November 30th and December 2nd, 2016, i.e. during the dry
142 season.

143 *Acer negundo* is deciduous and has leaves only during austral spring-summer (October-March).
144 *Olea europeae*, *Brachichyton populneus*, *Quillaja saponaria*, *Schinus molle*, *Cryptocaria alba*,
145 *Acacia caven* and *Maytenus boaria* are permanent. Moreover, *Q. saponaria* renews its leaves every
146 2-3 years. Because all trees in the AOMS group were planted in nov. 2014, they all have undergone
147 a similar exposure time of 2 years.

148

149 **II.2 Methods**

150 **II.2.1 Magnetic measurements**

151 The magnetic measurements were carried out with two objectives: to quantify the amount of
152 ferromagnetic minerals present in a sample and to obtain information about their nature and magnetic
153 grain size. The first objective can be attained with two kinds of measurements. The bulk magnetic
154 susceptibility (MS) is the magnetization acquired in a low field per unit field, normalized per weight.
155 In first approximation, MS depends on the concentration of magnetic minerals and is widely used to
156 quantify the amount of magnetic minerals. The Saturation Isothermal Remanent Magnetization
157 (SIRM) is the remanent magnetization (i.e., measured in zero-field) that a sample acquires after being
158 exposed to a magnetic field high enough to saturate its magnetization. Because the applied field is
159 high, the SIRM values are able to quantify a magnetic contribution even when the magnetic minerals
160 have a low concentration, as is the case in tree leaves.

161 The identification and magnetic grain size determination of magnetic minerals was addressed with
162 the measurement of hysteresis loops, which is the variation of magnetization with an applied field
163 (Fig. SI-1a). Another information is given by the acquisition of Isothermal Remanent Magnetization
164 (IRM) as a function of applied field, since the field required to saturate a magnetic mineral can be
165 different for different minerals (Fig. SI-1b). See SI for more details.

166 MS measurements were carried out using AGICO KLY-3 Kappabridge at Institut de Physique du
167 Globe, Paris. SIRM measurements were carried out using a Lakeshore Vibrating Sample
168 Magnetometer (VSM) at the IMPMC-IPGP Magnetic Mineral Analysis Facility. A field of 1 T was
169 applied, which is well above the saturating field measured for all our samples. Hysteresis loops and
170 IRM acquisition curves were also measured with the same instrument.

171

172 **II.2.2 PIXE measurements**

173 Particle Induced X-ray Emission (PIXE) is a technique for the elemental analysis of a sample, which
174 is used as a target for the bombardment with a beam of accelerated particles; the interactions of the
175 beam particles with the target atoms lead to the emission of X-rays of characteristic energies, through
176 the detection of which the target composition can be deduced. In this technique, protons are almost
177 universally chosen to induce X-ray emission (Lucarelli, 2020). *M. boaria*, *O. europea* (in two sample
178 sites), *Q. saponaria*, *S. molle*, *C. alba* and *B. populneus* leaves were analyzed for elemental
179 composition. *M. boaria*, and *O. europea* samples were measured from two other sites: an urban street
180 (Recoleta-Einstein) and a site within the Faculty. This latter site is on the Campus of the Faculty of
181 Chemical and Pharmaceutical Sciences of University of Chile (33.3° lat. S and 70.4° long. W), located
182 in Independencia commune in the city of Santiago; it has about 3 ha with small green areas and trees;
183 it is surrounded by tall buildings reaching until 60 m (20 floors) and was considered as a site that
184 should receive little exposure in PM. Leaves from *C. alba* were also sampled on this site. For each
185 tree species, three leaves cleaned and three leaves exposed were analyzed by PIXE on both surfaces:
186 adaxial (top) and abaxial (down). Leaves were washed following the method of Guerrero-Leiva et al.

187 (2016). Elemental quantification was done using Micromatter standards (with a 5% uncertainty).
188 Twenty-five elements were quantified on the samples: Na, Mg, Al, Si, P, S, Cl, K, Ca, Ti, V, Cr, Mn,
189 Fe, Ni, Cu, Zn, As, Se, Br, Rb, Y, Zr, Mo, Pb.

190 The spectra acquired show that clean leaves are quite homogeneous, while the deposition of PM
191 results in slight inhomogeneities that depend also on the leaves morphology such as veining and the
192 side of the leaf analyzed (Fig. SI-2).

193

194 **III. Results**

195 **III.1. Magnetic measurements on Recoleta sample group**

196 The magnetic properties of leaves of *A. negundo* and UD samples along Recoleta Avenue were
197 measured. The SIRM and MS values for the leaves samples show a large variation, ranging from 1.7
198 to 4.3×10^{-3} mAm²/kg for the SIRM and from 0.17 to 0.44×10^{-6} m³/kg for the MS (Fig. 2a, b). For
199 the UD samples, the SIRM values range from 45 to 85×10^{-3} mAm²/kg, and the MS values from 6.6
200 to 13.1×10^{-6} m³/kg (Fig. 2c, d).

201 There is a good correlation between SIRM and MS values for the leaf samples (*p-value*=0.000037),
202 indicating that the magnetic mineralogy is similar within the sample group (Fig.3a). The correlation
203 is less good for the UD samples (*p-value*=0.049) (Fig.3b). The similar magnetic mineralogy is further
204 confirmed by Day-plots: the hysteresis parameters are clustered in the pseudo-single-domain (PSD,
205 see Fig. SI-1)) region, with the UD samples slightly closer to the multidomain (MD) region than the
206 leaf samples, and slightly more dispersed (Fig. 3c).

207 The SIRM acquisition curves (Fig. SI-3) show that the SIRM is reached for all samples when the
208 applied field is around 0.3 T. This value is characteristic for magnetite-like minerals, which are the
209 expected Fe-rich particles from a vehicular source (e.g., Mitchell and Maher, 2009; Gonet and Maher,
210 2019).

211

212 **III.2. Magnetic particles and elemental composition on Mixed sample group**

213 The magnetic properties of leaves of *O. europeae*, *S. molle*, *A. caven*, *M. boaria*, *C. alba*, *B. populneus*
214 and *Q. saponaria* leaves and UD samples were measured. Because the leaves come from trees of
215 different species, the spatial cartography for this group of samples cannot be interpreted as a spatial
216 pollution monitoring tool, but it could be a useful screening tool. We measure SIRM values between
217 0.7 and 4.3×10^{-3} mAm²/kg and MS values between 0.08 and 0.48×10^{-6} m³/kg for the leaf samples
218 (Fig. SI-4a and b). For the corresponding UD samples, the SIRM values range from 60 to 163×10^{-3}
219 mAm²/kg and the MS values from 10.94 to 20.02×10^{-6} m³/kg (Fig. SI-4c and d). These values are in
220 the same order of magnitude as for the Recoleta Avenue samples group. The highest SIRM and MS
221 values are obtained for *O. europeae*, *S. molle* and *A. caven* leaves, while those values are much lower
222 for *M. boaria*, *C. alba*, *B. populneus* and *Q. saponaria* leaves.

223 The good correlation between SIRM and MS for all tree or UD samples (Fig. 3d, e), as well as the
224 similar hysteresis parameters (Fig. 3f) suggest that the magnetic mineralogy is consistent within the
225 sample set (*p-value*=0.000516 for the leaf samples and 0.00591 for the UD). The leaves hysteresis
226 parameters are slightly closer to the SD region than the UD parameters.

227 The SIRM acquisition curves show the same saturation field for all leaves and UD samples around
228 0.3 T, which is consistent with a magnetite-like value (Fig. SI-5). When comparing the SIRM or MS
229 of leaves with those of UD, we find that there is no correlation between both, indicating again that
230 the magnetic signal in UD and leaves do not have the same contributions, even though the magnetic
231 minerals have almost the same magnetic signature (Fig. SI-6).

232 In general, *O. europea* (Rec-B), *Q. saponaria* (Rec-E) and *M. boaria* (Rep-A) leaves present the
233 highest elemental concentration (Fig. 4a). The most predominant elements for most of the species are
234 Na, Al, Si, S, Cl, K, Mn, Fe, Cu, and Zn on urban street. Potassium, Cl, Fe and Cu are observed in
235 the three species on Faculty (Fig. 4b). The total elemental concentration for *O. europea* leaves at the
236 Rec-B site is 385 µg/cm² while that of leaves of the same species at the Rec-Z site is only 30 µg/cm²,
237 i.e. the Rec-B site collected ten times more PM (mainly Ca, K and Si) than the Rec-Z site (Si, Fe and
238 Cl). Magnesium, Al, Si, P, S, Cl, K, Ca, Ti, Mn, Fe, Cu, Br and Zn predominate in the abaxial side

239 of *O. europeae* at Rec-B site, while at Rec-Z site, S and Ca predominate in the adaxial side and Ti,
240 Mn, Fe and Br predominate in the abaxial side of the leaves.

241 *M. boaria* leaves present a total elemental concentration of 159 $\mu\text{g}/\text{cm}^2$ at Rep-A site and 177 $\mu\text{g}/\text{cm}^2$
242 on the Faculty sites. Chlorine, K and Si have the highest concentrations on Rep-A site leaves while
243 Ca, Si and Fe are predominant on leaves from Faculty site. Aluminium, Si, Ti, Fe, Cu and Zn are the
244 elements that are the most concentrated on the adaxial side of *M. boaria* leaves from Rep-A site,
245 while Al, Si, K, Ti, Fe and Cu are the most concentrated on the abaxial side of *M. boaria* leaves from
246 Faculty. *Q. saponaria* leaves have a concentration of 225 $\mu\text{g}/\text{cm}^2$ and 69 $\mu\text{g}/\text{cm}^2$ at Rec-E site and
247 Faculty site, respectively. The elements Ca, K and Fe are the most concentrated in Rec-E and K, Cl
248 and Fe in Faculty (Fig. 5a). Manganese and Fe are much more concentrated on the abaxial side of
249 leaves from Rec-E, while Mg and K are in higher concentration on the adaxial side. Manganese and
250 Fe are higher on the abaxial side, and Cl and Cu are present on both sides of leaves from Faculty. *C.*
251 *alba* leaves presented the same deposit at Por-M site as in Faculty 79 $\mu\text{g}/\text{cm}^2$ and 89 $\mu\text{g}/\text{cm}^2$,
252 respectively. Potassium, Cl and Si are the most concentrated at Por-M site and Faculty (Fig. 5b).
253 Magnesium, Al, Si, P, S, Cl, K, Mn, Fe, Ni, Cu, Zn and Se are on both sides of leaves in Rec-E, while,
254 Al, Si, P, Cl, K, Fe and Cu on Faculty.

255 *S. molle* (Rec-Z site) and *B. populneus* (Rec-E site) leaves had a total elemental concentration of 48
256 $\mu\text{g}/\text{cm}^2$ and 58 $\mu\text{g}/\text{cm}^2$, respectively. In *S. molle*, Si, As and Fe were the most predominant elements
257 (Fig. 4a), Sodium, Si, Cu, As and Pb are in higher concentration on the abaxial side and Mg, S, Cl,
258 Ti, V, Mn and Ni are higher on the adaxial side. Aluminum is similar on both sides. In *B. populneus*
259 Si, K and Fe were the most predominant elements, Na, Al, Si, Fe, Cu, Br and Pb are in higher
260 concentration on the abaxial side of leaves, K and Se are predominant on the adaxial side, and S, V,
261 Mn and Sr are similar on both sides.

262

263 **III-3- Air official monitoring stations (AOMS) group.**

264 Only *Q. saponaria* leaves were sampled for this sample set, close to AOMS distributed throughout
265 Santiago. SIRM and MS values are very weak compared with values from the other sample sets and
266 other similar studies. The SIRM values range between 0.20 and 0.42×10^{-3} mAm²/kg while the MS
267 values range between 0.02 and 0.07×10^{-6} m³/kg (Fig. 6).

268 Unlike the previous sample sets, there is no correlation between MS and SIRM values (*p-value* =
269 0.52), showing that the magnetic mineralogy is different within the sample set (Fig. 3g). This is
270 confirmed by the hysteresis parameters that are much more dispersed than in the previous data sets,
271 though mostly in the PSD region (Fig. 3h). SIRM acquisition curves are fairly noisy, since the
272 magnetic signal is very weak, nevertheless the saturation still happens around 0.3 T and shows a
273 predominance of a magnetite-like magnetization carrier (Fig. SI-7).

274

275 III- Discussion

276 1- General remarks about magnetic properties

277 All samples (leaves and UD) have a magnetic mineralogy consistent with magnetite-like minerals in
278 the PSD size range. This agrees with most other studies that used passive captors as urban pollution
279 proxy (e.g., Maher et al., 2008; Mitchell and Maher, 2009). The values recorded in leaves through
280 MS and SIRM are several times higher than the values measured by Muñoz et al. (2017) in Santiago
281 in *Platanus x acerifolia*, but the area covered in that study was probably traveled by newer private
282 vehicles that emit less PM than the busier areas sampled in this study. For UD samples, MS and SIRM
283 values are higher than the values of Aguilar et al. (2013) measured in Bogota, but the same order of
284 magnitude as the values of Muñoz et al. (2017), this time in the same area of Santiago than the one
285 studied here. Indeed, in Muñoz et al. (2017), two different type of communes, corresponding to two
286 different environments, were studied: one with newer private vehicles and less public vehicles and
287 the other one similar to group A of this study.

288 The Recoleta and the Mixed tree species sample sets also show that the magnetic particles deposited
289 on tree leaves have the same origin, unlike those found in soil. This could be caused by the fact that
290 the magnetic signal in UD also has a natural origin that is not so important on tree leaves, and
291 reinforces the conclusion that the leaves are better indicators of anthropogenic magnetic PM than UD.
292 The particles from the exhaust pipe of motor vehicles are mainly found in the fine fraction of the PM
293 and therefore, they are more easily deposited at a higher altitude than the larger particles that are more
294 abundant in the soil.

295

296 2- Recoleta group

297 The values measured in UD samples are the same order of magnitude as those measured in Recoleta
298 sector by Muñoz et al. (2017). The profile along Recoleta Avenue (*A. negundo*) is useful to identify
299 PM hotspots. For instance, the high values measured at the point R1, close to the subway station, can
300 be explained by the presence of a major intersection coupled with a bus hub. At point R7, the presence
301 of a car repair shop could cause the high values observed in this area. The results for the UD samples
302 are quite consistent with the results for the leaves. Urban dust collected at sites R1 and R7 also show
303 high values of SIRM. This sample set shows that important information could be gained from this
304 measurement type and could be used to issue recommendations for pedestrians. For instance, if such
305 measurements are carried out on sidewalk both sides of a street, it could lead to information as simple
306 as which side of the road is the best to walk on to minimize PM the exposition.

307

308 3- Mixed species group

309 The leaf samples show that, in decreasing order: *O. europeae* presents a high magnetic signal located
310 at the Rec-B site, followed by *S. molle* and *A. negundo* that are at the Rec-Z site, and followed by *A.*
311 *caven* located at the Ala-M site. All those streets have high vehicular traffic (highest in Alameda).
312 The values obtained with the *O. europeae* sampled at the Rec-Z site are weak, compared to those

313 obtained from *S. molle* at the same location and *O. europea* at Rec-B site; however, the signal from
314 *A. negundo* coincides with that recorded by *S. molle*.

315 In addition, samples of this group were analyzed by PIXE, providing the first background of elemental
316 composition leaves by this technique. Various elements were identified on both sides of the sample
317 leaves: Na, Al, Si, S, P, Cl, K, Ca, Ti, Cr, Mn, Fe, Cu, Zn, Rb, Mo and Pb. The identification of Fe is
318 consistent with the magnetic particle signals indicated. In the leaves samples from the Faculty site
319 (closed space) a lower proportion of some elements was observed. In general, the leaves of *O.*
320 *europeae* from the Rec-B site, *Q. saponaria* (Rec-E) and *M. boaria* (Rep-A) presented a higher
321 proportion of elements per surface area. This can be related to a greater proximity to the source of
322 emission and to the properties of the species that contribute to a greater capture of particles.

323 The high elemental concentration in *M. boaria* in the Faculty site could be explained by its proximity
324 to a construction site of a mall and a building, which could also explain the high Ca concentration. *C.*
325 *alba* leaves from the Faculty site shows similar elemental concentration compared to the leaves from
326 Por-M site.

327 There are two sites in this group of samples where two different trees are co-located: 1) *S.molle* and
328 *O. europeae* (Rec-Z) collecting a different concentration of PM with a different elemental
329 composition and distribution of the element on both sides of the leaves, however both collect heavy
330 metal as As, Mn Fe or Pb concentrated on the abaxial side. Magnetic parameters have higher values
331 for *S. molle* leaves than for *O. European* leaves, which seems consistent with the PM concentration
332 data. 2) *Q. saponaria* and *B. populneus* also collect very different concentration of PM and both
333 collect the heavy metals as Mn, Fe, Cu or Pb concentrated on the abaxial side of leaves. The
334 consistency of the elemental results with magnetic parameters is not as good, since they are very
335 similar for the leaves from both trees. These results show that the ability to retain PM is species-
336 specific.

337 The comparison between concentrations on the abaxial and adaxial sides shows that in general,
338 elemental concentrations are higher in the adaxial side. In particular, concentrations of elements

339 which are mainly in the coarse fraction (like crustal elements Al and Si, and abrasion element, such
340 as Fe) are higher in the adaxial side, which is compatible with a major contribution of settling as
341 removal process, while elements which are mainly in the fine fraction, such as S (secondary
342 particulate produced from SO₂), are found on both sides, which is compatible with a major
343 contribution of diffusion.

344 The elements detected have been previously identified in PM₁₀ and PM_{2.5} in cities. Some of them are
345 mainly linked to windblown soil resuspension or dust transport (e.g., Al, Si, Ti...), others to
346 anthropogenic emissions (e.g., Cu and Zn from vehicular brake and tire wear, dust from traffic
347 resuspension...). Pattanaik et al (2020) indicate that Zn as its speciation, coming from residual oil
348 combustion, varies through the different size fractions of PM and has implications on the
349 bioavailability and toxicity of Zn. Although some elements are specific markers for some sources,
350 most elements may have contributions from different sources and the quantification of such
351 contributions may be carried out only by using source apportionment studies (Amato et al., 2016,
352 Lucarelli et al., 2015).

353 We looked for possible correlations between the magnetic parameters (magnetic susceptibility and
354 SIRM) and the elemental concentrations. The correlation between total elemental concentrations and
355 magnetic parameters is weak ($R^2=0.36$ for SIRM and 0.42 for MS) and not significant at $p < 0.05$ (p -
356 $value = 0.15$ for SIRM and 0.12 for MS). Individual elements that are associated with magnetic PM
357 are Zn, Cd, Pb, Ni, Cu and Cr (Cao et al. 2015). Here, only Cu shows a weak correlation with magnetic
358 parameters ($R^2=0.49$ for SIRM and 0.61 for MS; p - $value = 0.08$ for SIRM and 0.04 for MS); the other
359 elements cited by Cao et al. (2015) either show no correlation with magnetic parameters or were not
360 measured in enough leaves samples to enable a meaningful correlation analysis. The other elements
361 that are correlated with magnetic parameters are S ($R^2=0.64$ for SIRM and 0.70 for MS; p - $value =$
362 0.02 both for SIRM and MS) and Br ($R^2=0.83$ for SIRM and 0.51 for MS, but p - $value = 0.09$ for
363 SIRM and 0.29 for MS).

364

365 4- AOMS group

366 The magnetic values obtained for all *Q. saponaria* leaves at AOMS have much lower values (almost
367 an order of magnitude) than those of all other samples measured. We only have one value other than
368 from this sample set for a *Q. saponaria* sample, and it is much higher than the AOMS values. There
369 might be an effect of the age of the individual trees that can affect the capture of PM (Préndez et al.,
370 2013): the *Q. saponaria* in the AOMS group are young compared to the other *Q. saponaria*. But it
371 could also suggest that the station locations might not be representative of the actual PM pollution
372 than most of the town of Santiago experiences, at least from traffic pollution. The magnetic particles
373 present on the leaves do not seem to have all the same origin as in the two other sample sets; since
374 the sampling sites are slightly further away from the roads, this may be an effect of a larger diversity
375 of sources of the anthropogenic component, that would not be limited to vehicular emissions but also
376 industrial emissions or-burning of biomass, or an effect of the smaller anthropogenic component,
377 which makes the natural component more visible; this component has a magnetic signature more
378 diverse than the anthropogenic component.

379 Because the PM that are responsible for the magnetic signal are deposited as well as integrated inside
380 the leaves, rainfall can affect the magnetic response, removing deposited PM on their surface by
381 washing (Mitchell and Maher, 2009; Matzka and Maher, 1999; Castaneda-Miranda et al., 2020). The
382 rainy season in Santiago takes place from April until September, so outside of the sampling period.
383 Moreover, we did not try to compare the different values. Rather, we obtained information about the
384 order of magnitude in the magnetic signal and information about the diversity of provenance of
385 magnetic PM; these two pieces of information are less affected by rainfalls than a true quantitative
386 comparison between sites.

387 In order to extend these observations to the level of individual trees, the foliar surface of each tree
388 must be considered. Calculations of the Leaf Area Index (LAI) of individual trees cover are in
389 progress, in order to estimate the effective removal of PM from vehicle emissions by different tree
390 species in Santiago.

391 Similar studies about the mitigating function of trees could be replicated in other cities of Chile,
392 keeping in mind other criteria such as restriction/abundance of soil, or water and space conditions.
393 Such studies will help in the elaboration of strategies for future urban climate scenarios.

394

395 **IV- Conclusions**

396 We have carried out a magnetic and elemental study on tree leaves as well as a magnetic study on
397 UD in Santiago, Chile. The main results are the following:

- 398 - Magnetic signal measured on urban tree leaves is a good proxy for tracing anthropogenic
399 metallic particles, while similar measurements on urban soil may be more influenced by
400 particles of detritic (natural) origin.
- 401 - Magnetic measurements on tree leaves can be used in spatially localized studies in cities to
402 help identify PM hotspots, thanks to the excellent spatial resolution of this technique.
- 403 - Elemental PIXE analysis of tree leaves allows to quantify many elements associated with
404 vehicular emissions. Copper, Zn, Fe, K and S are present on every site, while As, Se, V, Ni,
405 Sr, Zr, Mo and Pb are identified on some sites. This technique can also distinguish the
406 elemental composition on both sides of the leaves.
- 407 - The results obtained reinforce the role of trees as specie-specific biomonitors in the capture
408 of PM in terms of quantity and quality of the material removed from the atmosphere,
409 depending on the environment surrounding the plant.

410

411

412 **Acknowledgements**

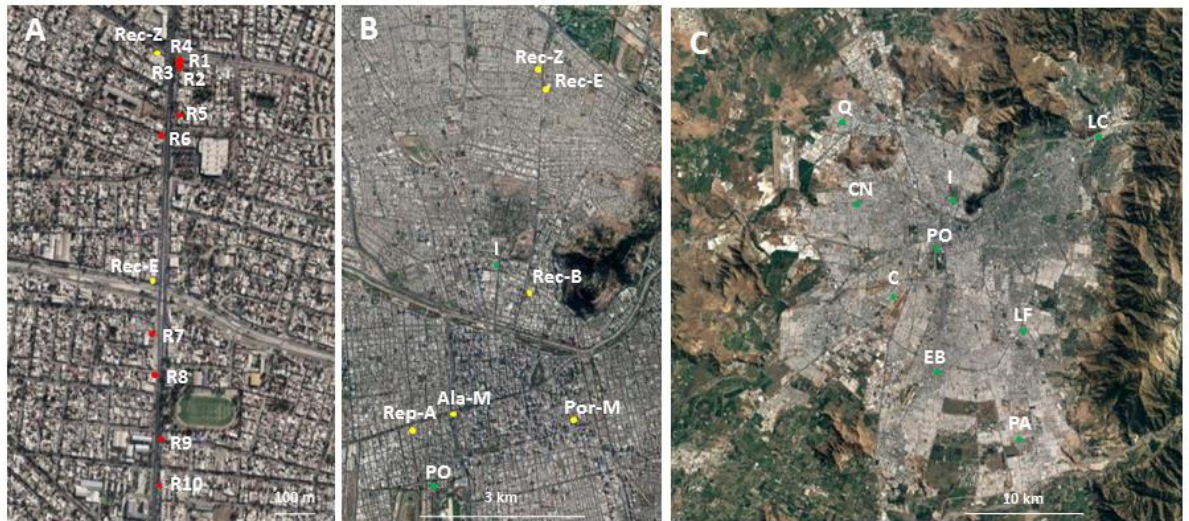
413 Authors acknowledge funding from project URedes Consolidación-URC-026/17, VID, Universidad
414 de Chile.

415

416 **Figures**

417

418



419

420 **Fig. 1** Samples group locations. A: Recoleta sample group: location of ten specific *Acer negundo*

421 individuals on Recoleta Avenue (red markers). B: Mixed sample group: Location of eight urban tree

422 species in Santiago. The locations of the intersections are: Rec-Z: Recoleta/Zapadores; Rec-E:

423 Recoleta/Einstein; Rec-B: Recoleta/Buenos Aires; Ala-M: Alameda/Manuel Rodriguez; Rep-A:

424 Republica/Alameda; Por-M: Portugal/Alameda C: AOMS sample group: Location of nine *Quillaja*

425 *saponaria* individuals installed in the Air Quality Monitoring Stations, Santiago. The locations of the

426 sites are: PA: Puento Alto; EB: El Bosque; C: Cerillos; PO: Parque O’Higgins; CN: Cerro Navia; LC:

427 Las Condes, LF: La Florida; I: Independencia; Q: Quilicura

428



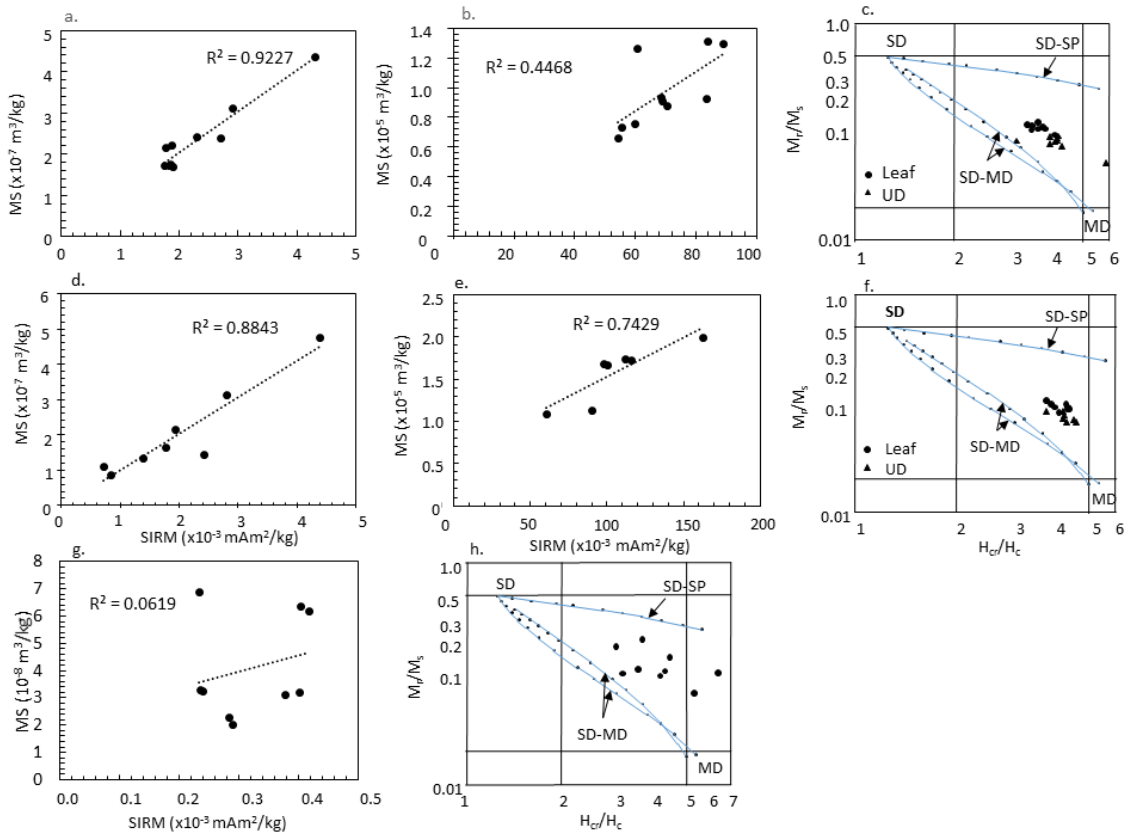
430

431 **Fig. 2** Cartography of magnetic parameters for leaves (a. SIRM; b. magnetic susceptibility) and urban

432 dust (c. SIRM; d. magnetic susceptibility) for the samples taken along Recoleta Avenue (Recoleta

433 sample group)

434



435

436 **Fig. 3** Magnetic properties of samples from Recoleta, Mixed and AOMS samples group. Correlation

437 between SIRM and MS values for a: leaf samples; b: urban dust samples from Recoleta Avenue; c:

438 Day-plot for the Recoleta Avenue samples; Correlation between SIRM and MS values for d: leaf

439 samples; e: urban dust samples from the Mixed species samples; f: Day-plot for the Mixed Species

440 samples (SD: single-domain; SP: superparamagnetic; MD: multidomain); g: correlation between

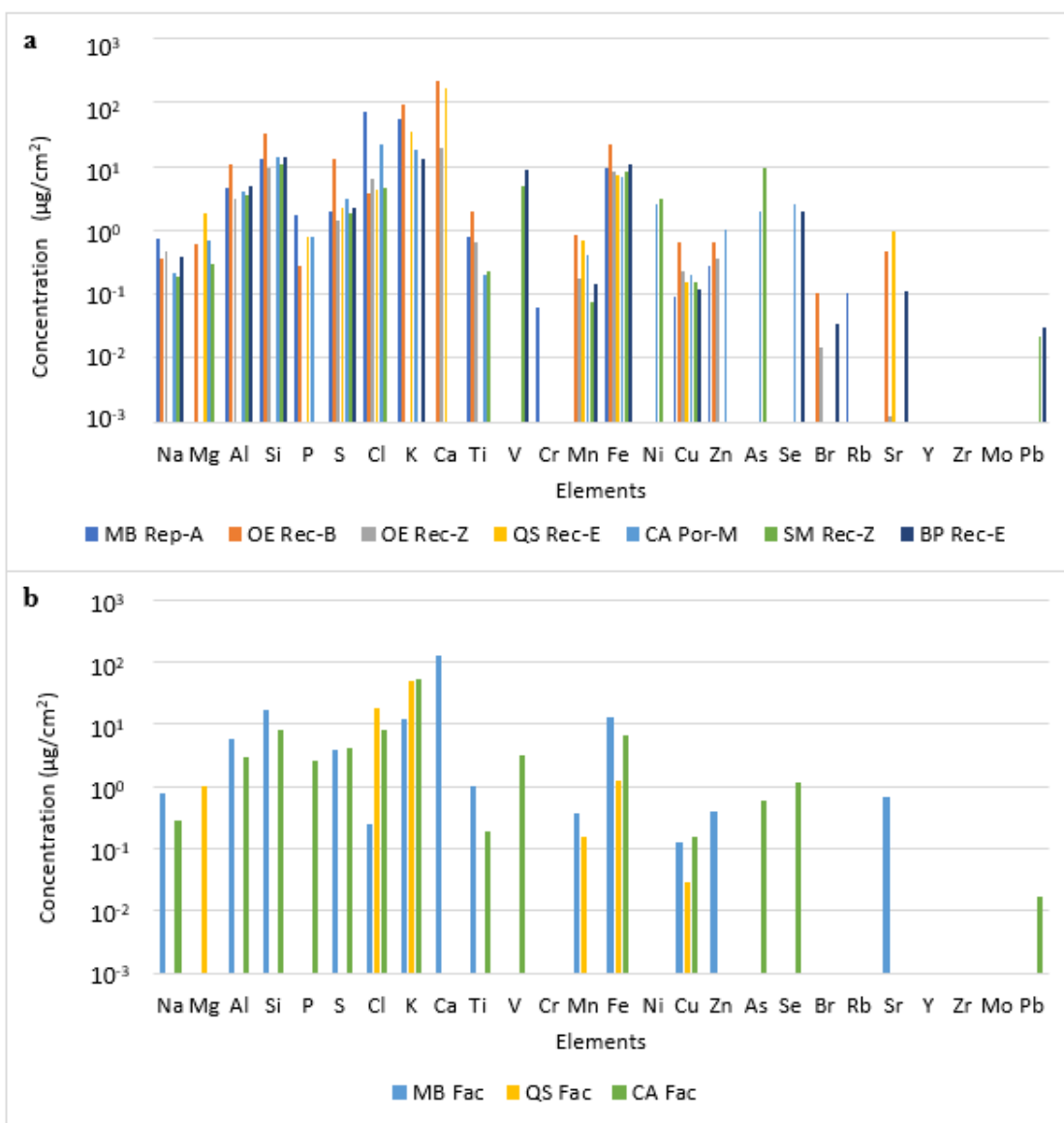
441 SIRM and MS values for leaf samples from AOMS sample group; h: Day-plot for the AOMS sample

442 group

443

444

445



446

447

448

449

450

451

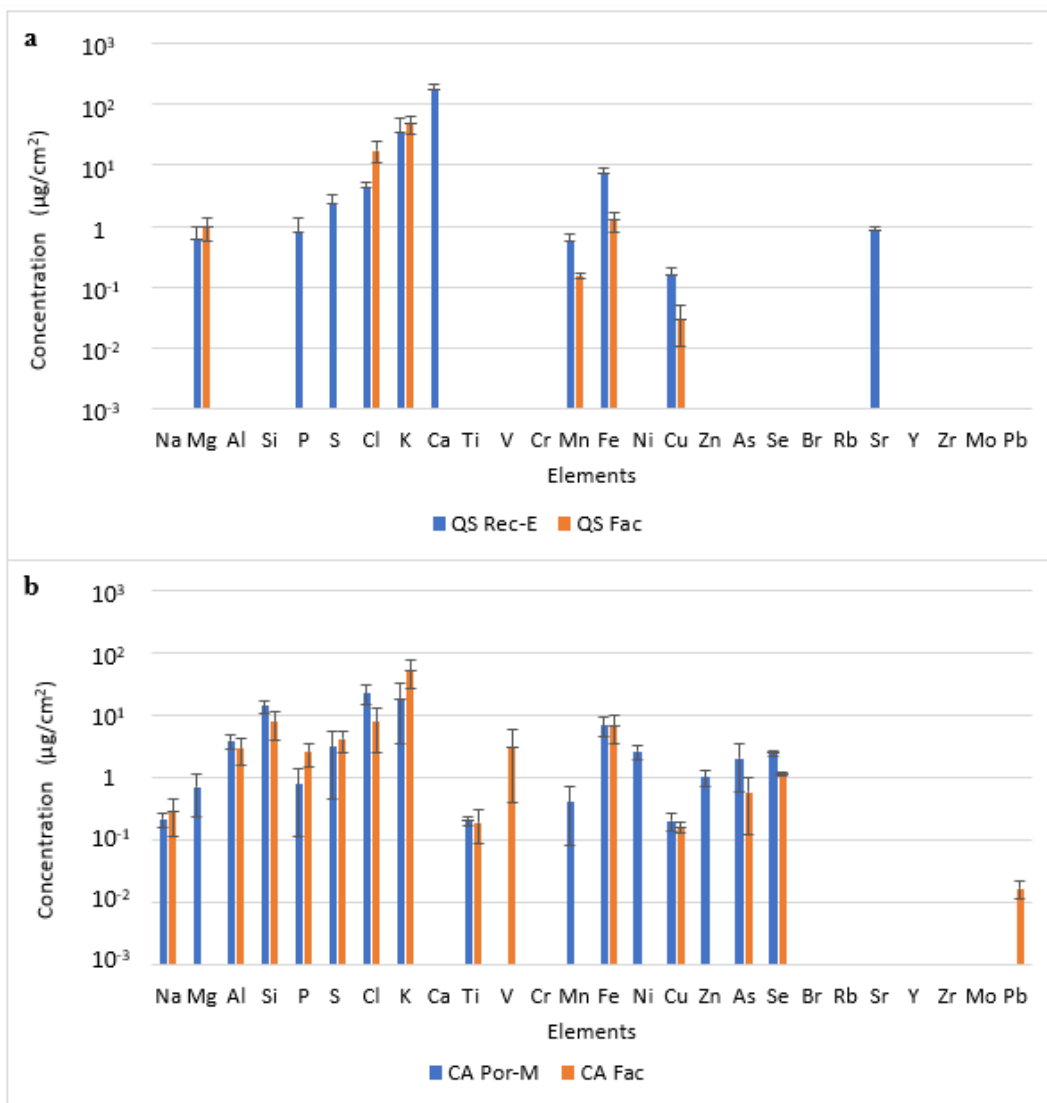
452

Fig. 4 Elemental concentration on: a. leaves of *Maytenus boaria* at Republica/Alameda (MB Rep-A), *Olea europea* at Recoleta/Buenos Aires (OE Rec-B) and at Recoleta/Zapadores (OE Rec-Z), *Quillaja saponaria* at Recoleta/Einstein (QS rec-E) , *Cryptocaria alba* at Portugal/Marin (CA Por-M), *Schinus molle* at Recoleta/Zapadores (SM Rec-Z), and *Brachichiton populneus* at Recoleta-Einstein (BP Rec-E); b: *Maytenus boaria* (MB Fac), *Quillaja saponaria* (QS Fac) and *Cryptocaria alba* (CA Fac) leaves on Faculty site

453

454

455

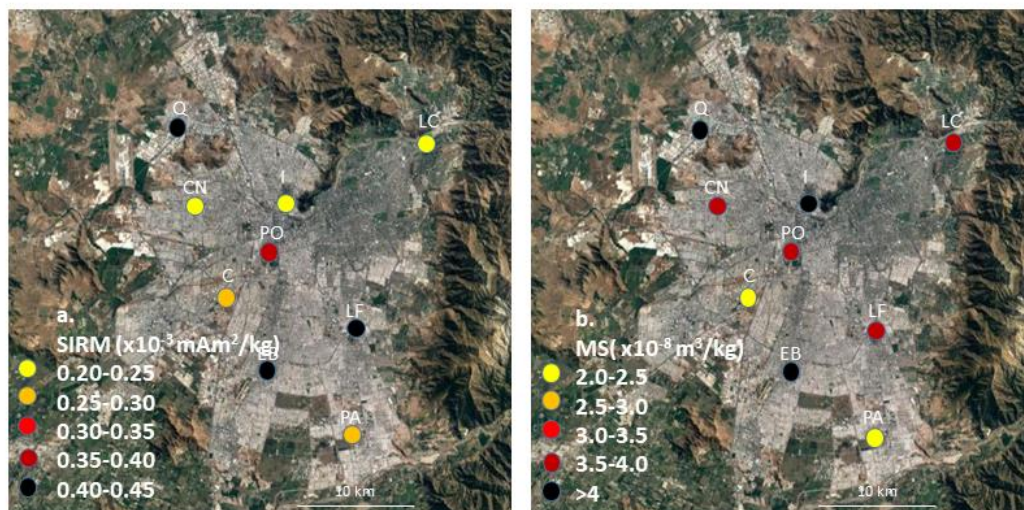


456

457 **Fig. 5** Elemental concentration and standard deviation for: a. *Quillaja saponaria* (QS) leaves at
458 Recoleta-Einstein (Rec-E) and Faculty (Fac) sites; b. *Cryptocarya alba* (CA) leaves at Portugal-
459 Marin (Por-M) and Faculty (Fac) sites

460

461



462

463 **Fig. 6** Cartography of magnetic parameters for leaves from AOMS sample group (a. SIRM; b.

464 magnetic susceptibility)

465

466

467

468 **References:**

469 Aguilar Reyes, B., Bautista, F., Gogichaishvili, A., & Morton, O. (2011). Magnetic monitoring of top
470 soils of Merida (southern Mexico). *Studia Geophysica et Geodaetica*, 55, 377-388.

471 Aguilar Reyes, B., Cejudo Ruiz, R., Martínez-Cruz, J., Bautista, F., Goguitchaichvili, A., Carvallo,
472 C., & Morales, J. (2012): Ficus benjamina leaves as indicator of atmospheric pollution: a
473 reconnaissance study. *Studia Geophysica et Geodaetica*, 56, 879–887.
474 <https://doi.org/10.1007/s11200-011-0265-1>

475 Aguilar, B.O., Mejia, V., Goguitchaichvili, A., Escobar, J., Bayona, G., Bautista, F., Morales, J.J., &
476 Ihl, T.J. (2012). Reconnaissance environmental magnetic study of urban soils, dust and leaves
477 from Bogotá, Colombia. *Studia Geophysica et Geodaetica*, 57, 741– 754.
478 <https://doi.org/10.1007/s11200-012-0682-9>

479 Amato, F., Alastuey, A., Karanasiou, A., Lucarelli, F., Nava, S., Calzolari, G., Severi, M., Becagli, S.,
480 Gianelle, V.L., Colombi, C., Alves, C., Custódio, D., Nunes, T., Cerqueira, M., Pio, C.,
481 Eleftheriadis, K., Diapouli, E., Reche, C., Minguillón, M.C., Manousakas, M.-I., Maggos, T.,
482 Vratolis, S., Harrison, R.M., & Querol, X. (2016). AIRUSE-LIFE+: a harmonized PM
483 speciation and source apportionment in five southern European cities. *Atmospheric Chemistry*
484 *and Physics*, 16, 3289–3309. <https://doi.org/10.5194/acp-16-3289-2016>

485 Araya, M., Seelenfreund, D., Buscaglia, M., Peña-Ahumada, B., Vera, J., Egas, C., & Préndez, M.
486 (2019). Assessment of Anthropogenic Volatile Organic Compounds in Leaves of Two Urban
487 Tree Species in Santiago de Chile. *Frontiers in Forests and Global Change*, 2, 42.
488 <https://doi.org/10.3389/ffgc.2019.00042>

489 Buccolieri, R., Sandberg, M., & Di Sabatino, S. (2010): City breathability and its link to pollutant
490 concentration distribution within urban-like geometries. *Atmospheric Environment*, 44, 15,
491 1894-1903. <https://doi.org/10.1016/j.atmosenv.2010.02.022>

492 Cao, L., Appel, E., Hu, S., Yin, G., Lin, H., & Rösler, W. (2015). Magnetic response to air pollution
493 recorded by soil and dust-loaded leaves in a changing industrial environment. *Atmospheric*
494 *Environment*, 119, 304-313. <https://doi.org/10.1016/j.atmosenv.2015.06.017>

495 Castaneda-Miranda, A.G., Chaparro Marcos, A.E., Pacheco-Castro, A., Chaparro Mauro, A.E., &
496 Böhnel, H.N. (2020). Magnetic biomonitoring of atmospheric dust using tree leaves of *Ficus*
497 *benjamina* in Querétaro (Mexico). *Environmental Monitoring Assessment*, 192, 382.
498 <https://doi.org/10.1007/s10661-020-8238-x>

499 Castaneda-Miranda, A.G., Chaparro, M.A.E., Böhnel, H.E., Chaparro, M.A.E., Castaneda-Miranda,
500 R., Pacheco-Castro, A., Martinez-Fierro, M.L., Solis-Sanchez, L.O., & Ornela-Vargas, G.
501 (2021). *Bursera fagaroides* bark as a bioindicator for air particle pollution using magnetic
502 properties, *Journal of South American Earth Sciences*, 108, 103217.

503 Chaparro, M.A.E., Lavernia, J.M., Chaparro, M.A.E., & Sinito, A.M. (2013). Biomonitoring of urban
504 air pollution: magnetic studies and SEM observations of corticolous foliose and microfoliose
505 lichens and their suitability for magnetic monitoring. *Environmental Pollution*, 172, 61–69.
506 <https://doi.org/10.1016/j.envpol.2012.08.006>

507 Coccini, T., Caloni, F., Cando, L. J. R., & De Simone, U. (2017): Cytotoxicity and proliferative
508 capacity impairment induced on human brain cell cultures after short- and long-term exposure
509 to magnetite nanoparticles. *Journal of Applied Toxicology*, 37, 3, 361-373.
510 <https://doi.org/10.1002/jat.3367>

511 Costa, L. G., Cole, T. B., Coburn, J., Chang, Y.-C., Dao, K., & Roque, P. (2014). Neurotoxicants are
512 in the air: Convergence of human, animal, and in vitro studies on the effects of air pollution
513 on the brain. *BioMed Research International*, 736385. <https://doi.org/10.1155/2014/736385>

514 Costanza, R., Fisher, B., Mulder, K., Liu, S., & Christopher, T. (2007): Biodiversity and ecosystem
515 services: A multi-scale empirical study of the relationship between species richness and net

516 primary production. *Ecological Economics*, 61, 2-3, 478-491.
517 <https://doi.org/10.1016/j.ecolecon.2006.03.021>

518 Dzierzanowski, K., Popek, R., Gawronska, H., Saebo, A., & Gawronski, S.W. (2011). Deposition of
519 particulate matter of different size fractions on leaf surfaces and in waxes of urban forest
520 species. *International Journal of Phytoremediation*, 13, 1037–1046.
521 <https://doi.org/10.1080/15226514.2011.552929>

522 Egas, C., Bown, H., Godoy, N., Hernández, H.J., Naulin, P., Ponce, M. & Préndez, M. (2020).
523 Pollution induced leaf morphoanatomical changes of *Quillaja saponaria* in Santiago, Chile.
524 *Austin Environmental Sciences*, 5, 1, 1041.

525 Gonet, T., & Maher, B.A. (2019). Airborne, vehicle-derived Fe-bearing nanoparticles in the urban
526 environment: a review. *Environmental Science and Technology*, 53, 9970-9991.

527 Gramsch, E., López, G., Gidhagen, L., Segersson, D., Castillo, M., Vásquez, Y., Valverde, C., Díaz,
528 X., Tagle, M., & Donoso, R. (2014). Actualización y sistematización del inventario de
529 emisiones de contaminantes atmosféricos en la Región Metropolitana. pp. 34-52.

530 Guerrero-Leiva, N., Castro, S.A., Rubio, M.A., & Ortiz-Calderon, M. (2016): Retention of
531 Atmospheric Particulate by Three Woody Ornamental Species in Santiago, Chile. *Water Air
532 & Soil Pollution*, 227, 435. <https://doi.org/10.1007/s11270-016-3124-4>

533 Hernández, H.J., & Villaseñor, N.R. (2018): Twelve-year change in tree diversity and spatial
534 segregation in the Mediterranean city of Santiago, Chile. *Urban Forestry & Urban Greening*,
535 29, 10-18. <https://doi.org/10.1016/j.ufug.2017.10.017>

536 Hofman, J., Stokkaer, I., Snauwaert, L., & Samson, R. (2013): Spatial distribution assessment of
537 particulate matter in an urban street canyon using biomagnetic leaf monitoring of tree crown
538 deposited particles. *Environmental Pollution*, 183, 123-132.
539 <https://doi.org/10.1016/j.envpol.2012.09.015>

540 Karner, A. A., Eisinger, D. S., & Niemeier, D. A. (2010). Near-Roadway Air Quality: Synthesizing
541 the Findings from Real-World Data. *Environmental Science & Technology*, 44, 14, 5334-
542 5344. <https://doi.org/10.1021/es100008x>

543 Kelly, K., Whitaker, J., Petty, A., Widmer, C., Dybwad, A., Sleeth, D., & Butterfield, A. (2017).
544 Ambient and laboratory evaluation of a low-cost particulate matter sensor. *Environmental*
545 *Pollution*, 221, 491-500. <https://doi.org/10.1016/j.envpol.2016.12.039>

546 Kim, H., Liu, S., Russell, L.M., & Paulson, S.E. (2014). Dependence of Real Refractive Indices on
547 O:C, H:C and Mass Fragments of Secondary Organic Aerosol Generated from Ozonolysis
548 and Photooxidation of Limonene and alpha-Pinene. *Aerosol Science and Technology*, 48,
549 498-507. <https://doi.org/10.1080/02786826.2014.893278>

550 Liu, J.-Y., Hsiao, T.-C., Lee, K.-Y., Chuang, H.-C., Cheng, T.-J., & Chuang, K.-J. (2018).
551 Association of ultrafine particles with cardiopulmonary health among adult subjects in the
552 urban areas of northern Taiwan. *Science of the Total Environment*, 627, 211-215.
553 <https://doi.org/10.1016/j.scitotenv.2018.01.218>

554 Lucarelli, F. (2020). How a small accelerator can be useful for interdisciplinary applications: the study
555 of air pollution. *European Physical Journal Plus*, 135, 7, 53.
556 <https://doi:10.1140/epjp/s13360-020-00516-3>

557 Lucarelli, F., Nava, S., Calzolari, G., Chiari, M., Giannoni, M., Traversi, R., & Udisti, R. (2015). On
558 the autarchic use of solely PIXE data in particulate matter source apportionment studies by
559 receptor modeling. *Nuclear Instruments and Methods in Physics Research Section B: Beam*
560 *Interactions with Materials and Atoms* 363, 105-111.
561 <https://doi.org/10.1016/j.nimb.2015.08.019>

562 Lun, X., Lin, Y., Chai, F., Fan, C., Li, H., & Liu, J. (2020). Reviews of emission of biogenic volatile
563 organic compounds (BVOCs) in Asia. *Journal of Environmental Sciences*, 95, 266-277.
564 <https://doi.org/10.1016/j.jes.2020.04.043>

565 Maher, B.A., Moore, C., & Matzka, J. (2008). Spatial variation in vehicle-derived metal pollution
566 identified by magnetic and elemental analysis of roadside tree leaves. *Atmospheric*
567 *Environment*, 42, 364–373.

568 Malik, A.O., Jones, P.G., Chan, P.S., Peri-Okonny, P.A., Hejjaji, V., & Spertus, J.A. (2019).
569 Association of long-term exposure to particulate matter and ozone with health status and
570 mortality in patients after myocardial infarction. *Circulation: Cardiovascular Quality and*
571 *Outcomes* 12, e005598. <https://doi.org/10.1161/CIRCOUTCOMES.119.005598>

572 Manes, F., Marando, F., Capotorti, G., Blasi, C., Salvatori, E., Fusaro, L., Ciancarella, L., Mircea,
573 M., Marchetti, M., Chirici, G., & Munafò, M. (2016). Regulating Ecosystem Services of
574 forests in ten Italian Metropolitan Cities: Air quality improvement by PM₁₀ and O₃ removal.
575 *Ecological Indicators*, 67, 425–440. <https://doi.org/10.1016/j.ecolind.2016.03.009>

576 Marié, D.C., Chaparro, M.A.E., Irurzun, M.A., Lavornia, J.M., Marinelli, C., Cepeda, R., Böhnelt,
577 H.N., Castaneda-Miranda, A.G., & Sinito, A.M. (2016). Magnetic mapping of air pollution
578 in Tandil city (Argentina) using the lichen *Parmotrema pilosum* as biomonitor. *Atmospheric*
579 *Pollution Research*, 7, 513–520. <https://doi.org/10.1016/j.apr.2015.12.005>

580 Matzka, J., & Maher, B.A. (1999). Magnetic biomonitoring of roadside tree leaves: identification of
581 spatial and temporal variations in vehicle-derived particulates, *Atmospheric Environment*, 33,
582 28, 4565-4569.

583 Mitchell, R., & Maher, B.A. (2009). Evaluation and application of biomagnetic monitoring of traffic-
584 derived particulate pollution. *Atmospheric Environment*, 43, 13, 2095-2103.
585 <https://doi.org/10.1016/j.atmosenv.2009.01.042>

586 Moreno, E., Sagnotti, L., Dinarès-Turell, J., Winkler, A., & Cascella, A. (2003). Biomonitoring of air
587 traffic pollution in Rome using magnetic properties of tree leaves. *Atmospheric Environment*,
588 37, 21, 3967-2977. [https://doi.org/10.1016/S1352-2310\(03\)00244-9](https://doi.org/10.1016/S1352-2310(03)00244-9)

589 Muñoz, D., Aguilar, B., Fuentealba, R., & Préndez, M. (2017). Environmental studies in two
590 communes of Santiago de Chile by the analysis of magnetic properties of particulate matter

591 deposited on leaves of roadside trees. *Atmospheric Environment*, 152, 617-627.
592 <https://doi.org/10.1016/j.atmosenv.2016.12.047>

593 Nowak, D.J., Hirabayashi, S., Doyle, M., McGovern, M., & Pasher, J. (2018). Air pollution removal
594 by urban forests in Canada and its effect on air quality and human health. *Urban Forestry &*
595 *Urban Greening*, 29, 40-48. <https://doi.org/10.1016/j.ufug.2017.10.019>

596 Ottel , M., van Bohemen, H.D., & Fraaij, A.L.A. (2010). Quantifying the deposition of particulate
597 matter on climber vegetation on living walls. *Ecological Engineering*, 36, 2, 154–162.
598 <https://doi.org/10.1016/j.ecoleng.2009.02.007>

599 Pattanaik, S., & Huggins, F.E. (2020). Chemical nature of zinc in size fractionated particulate matter
600 from residual oil combustion - A comparative study. *Atmospheric Environment*, 221, 117099.
601 <https://doi.org/10.1016/j.atmosenv.2019.117099>

602 Ponce, M., Vallejos, O., & Mendoza, M. (2016). Contribuci n del arbolado urbano a la mitigaci n
603 del cambio clim tico. Medici n de las principales variables. Informe Final Proyecto NAC-I-
604 035-2014. Ministerio del Medio Ambiente de Chile. 24p.

605 Pope, C. A., & Dockery, D. W. (2006). Health Effects of Fine Particulate Air Pollution: Lines that
606 Connect. *Journal of the Air & Waste Management Association*, 56, 6, 709-742.
607 <https://doi.org/10.1080/10473289.2006.10464485>

608 Pr ndez, M., Araya, M., Criollo, C., Egas, C., Far as, I., Fuentealba, R., & Gonz lez, E. (2017). Urban
609 trees and its relationships with air pollution by particulate matter and ozone in Santiago,
610 Chile. In: C. Henr quez & H. Romero (eds), *Urban Climate in Latin-American Cities*.
611 Springer, Cham. https://doi.org/10.1007/978-3-319-97013-4_8

612 Pr ndez, M., Corada, K., & Morales, J. (2014). Natural organic compounds from the urban forest of
613 the Metropolitan Region, Chile: impact on air quality. In: K. Chetehouna (ed), *Volatile*
614 *Organic Compounds*. Nova Sciences Publishers Inc, New York pp. 103-142.

615 Préndez, M., Corada, K., & Morales, J. (2013). Emission factors of biogenic volatile organic
616 compounds in various stages of growth present in the urban forest of the Metropolitan Region,
617 Chile. *Research Journal of Chemistry and Environment*, 17, 11, 108-116.

618 Préndez, M., Alvarado, G., & Serey, I. (2011). Some Guidelines to Improve Air Quality Management
619 in Santiago, Chile: from Commune to Basin level. In: N. Mazzeo (Ed.), *Air Quality*
620 *Monitoring, Assessment and Management*. InTech, Rijeka, Croatia. pp. 305–328.

621 Ren, Y., Qu, Z., Du, Y., Xu, R., Ma, D., Yang, G., Shi, Y., Fan, X., Tani, A., Guo, P., & Chang,
622 J. (2017). Air quality and health effects of biogenic volatile organic compounds emissions
623 from urban green spaces and the mitigation strategies. *Environmental Pollution*, 230, 849-
624 861. <https://doi.org/10.1016/j.envpol.2017.06.049>

625 Roeland, S., Moretti, M., Amorim, J.H., Branquinho, C., Fares, S., Morelli, F., Niinemets, Ü.,
626 Paoletti, E., Pinho, P., Sgrigna, G., Stojanovski, V., Tiwary, A., Sicard, P., & Calfapietra, C.
627 (2019). Towards an integrative approach to evaluate the environmental ecosystem services
628 provided by urban forest. *Journal of Forestry Research*, 30, 1981–1996.
629 <https://doi.org/10.1007/s11676-019-00916-x>

630 Schulze, B.C., Wallace, H.W., Flynn, J.H., Lefer, B.L., Erickson, M.H., Jobson, B.T., Dusanter, S.,
631 Griffith, S.M., Hansen, R.F., Stevens, P.S., VanReken, T., & Griffin, R.J. (2017). Differences
632 in BVOC oxidation and SOA formation above and below the forest canopy. *Atmospheric*
633 *Chemistry and Physics*, 17, 3, 1805–1828. <https://doi.org/10.5194/acp-17-1805-2017>

634 Song, Y., Maher, B. A., Li, F., Wang, X., Sun, X., & Zhang, H. (2015).: Particulate matter deposited
635 on leaf of five evergreen species in Beijing, China: Source identification and size distribution.
636 *Atmospheric Environment*, 105, 53-60. <https://doi.org/10.1016/j.atmosenv.2015.01.032>

637 Toro, R., Morales, R., Canales, S., Gonzalez-Rojas, C., & Leiva, M. (2014). Inhaled and inspired
638 particulates in Metropolitan Santiago Chile exceed air quality standards. *Building and*
639 *Environment*, 79, 115–123. <https://doi.org/10.1016/j.buildenv.2014.05.004>

640 Tsai, D., Riediker, M., Berchet, A., Paccaud, F., Waeber, G., Vollenweider, P., & Bochud, M. (2019).
641 Effects of short- and long-term exposures to particulate matter on inflammatory marker levels
642 in the general population. *Environmental Science and Pollution Research*, 26, 19697–19704.
643 <https://doi.org/10.1007/s11356-019-05194-y>

644 Viecco, M., Vera S., Jorquera, H., Bustamante, W., Gironás, J., Dobbs, C., & Leiva, E. (2018).
645 Potential of particle matter dry deposition on green roofs and living walls vegetation for
646 mitigating urban atmospheric pollution in semiarid climates. *Sustainability*, 10, 7, 2431.
647 <https://doi.org/10.3390/su10072431>.

648 Wang, X. (2013). Heavy Metals in Urban Soils of Xuzhou, China: Spatial Distribution and
649 Correlation to Specific Magnetic Susceptibility. *International Journal of Geosciences*, 4,
650 309-316. <https://doi.org/10.4236/ijg.2013.42029>

651 Weichenthal, S., Bai, L., Hatzopoulou, M., van Ryswyk, K., Kwong, J.C., Jerrett, M., van Donkelaar,
652 A., Martin, R. V., Burnett, R.T., Lu, H., & Chen, H. (2017). Long-term exposure to ambient
653 ultrafine particles and respiratory disease incidence in 825 Toronto, Canada: a cohort study.
654 *Environmental Health*, 16, 64, 2017. <https://doi.org/10.1186/s12940-017-0276-7>

655 Weitekamp, A., Stevens, T., Stewart, M.J., Bhave, P., & Gilmour, I. (2020). Health effects from
656 freshly emitted versus oxidatively or photochemically aged air pollutants. *Science of The*
657 *Total Environment*, 704, 135772. <https://doi.org/10.1016/j.scitotenv.2019.135772>

658 Yang, P., Ge, J., & Yang, M. (2017). Identification of heavy metal pollution derived from traffic in
659 roadside soil using magnetic susceptibility. *Bulletin of Environmental Contamination and*
660 *Toxicology*, 98, 837–844. <https://doi.org/10.1007/s00128-017-2075-9>

661 Zikova, N., Hopke, P. K., & Ferro, A. R. (2017). Evaluation of new low-cost particle monitors for
662 PM_{2.5} concentrations measurements. *Journal of Aerosol Science*, 105, 24–34.
663 <https://doi.org/10.1016/j.jaerosci.2016.11.010>

664